Developmental Biology 321 (2008) 263–272

Contents lists available at ScienceDirect

Developmental Biology

journal homepage: www.elsevier.com/developmentalbiology

Grhl3 and *Lmo4* play coordinate roles in epidermal migration

Nikki R. Hislop [a], Jacinta Caddy [a], Stephen B. Ting [a], Alana Auden [a], Sumitha Vasudevan [a], Sarah L. King [a], Geoffrey J. Lindeman [b], Jane E. Visvader [b], John M. Cunningham [c], Stephen M. Jane [a,d,*]

[a] *Rotary Bone Marrow Research Laboratories, Melbourne Health Research Directorate, c/o Royal Melbourne Hospital Post Office, Parkville, VIC 3050, Australia*
[b] *Walter and Eliza Hall Institute for Medical Research, 1G Royal Parade, Parkville, Victoria, 3050, Australia*
[c] *Department of Pediatrics, and Institute of Molecular Pediatric Sciences, University of Chicago, Chicago IL 60637, USA*
[d] *Department of Medicine, University of Melbourne, Parkville VIC 3050, Australia*

ARTICLE INFO

Article history:
Received for publication 24 December 2007
Revised 28 May 2008
Accepted 18 June 2008
Available online 26 June 2008

Keywords:
Grainy head-like 3
Lmo4
Eyelid closure
Neural tube closure
Skin barrier

ABSTRACT

In addition to its role in formation of the epidermal barrier, the mammalian transcription factor *Grainy head*-like 3 (*Grhl3*) is also essential for neural tube closure and wound repair, processes that are dependent in part on epidermal migration. Here, we demonstrate that the LIM-only domain protein, LMO4 serves as a functional partner of GRHL3 in its established roles, and define a new cooperative role for these factors in another developmental epidermal migration event, eyelid fusion. GRHL3 and LMO4 interact biochemically and genetically, with mutant mice exhibiting fully penetrant exencephaly, thoraco-lumbo-sacral spina bifida, defective skin barrier formation, and a co-incident eyes-open-at-birth (EOB) phenotype, which is not observed in the original individual null lines. The two genes are co-expressed in the surface ectoderm of the migrating eyelid root, and electron microscopy of *Grhl3*/*Lmo4*-null eyes reveals a failure in epithelial extension and a lack of peridermal clump formation at the eyelid margins. Accumulation of actin fibers is also absent in the circumference of these eyelids, and ERK1/2 phosphorylation is lost in the epidermis and eyelids of $Grhl3^{-/-}/Lmo4^{-/-}$ embryos. Keratinocytes from mutant mice fail to "heal" in *in vitro* scratch assays, consistent with a general epidermal migratory defect that is dependent on ERK activation and actin cable formation.

Introduction

A key regulatory gene required for *Drosophila* development encodes the transcription factor *grainy head* (*grh*, also termed Elf-1 and NTF-1) (Bray et al., 1989; Bray and Kafatos, 1991). *Drosophila grh* is expressed predominantly in the surface ectoderm, where it plays essential roles in cuticle formation (Bray and Kafatos, 1991; Ostrowski et al., 2002) and wound repair (Mace et al., 2005). *Grh* has also been shown to be critical for dorsal closure (Attardi et al., 1993), which serves as a paradigm for epithelial morphogenetic events, including neural tube closure and wound healing in vertebrates (Jacinto et al., 2002). Our laboratory has recently identified a family of three mammalian developmental genes (*Grainy head-like 1-3, Grhl1-3*) that are highly related to *grh* (Wilanowski et al., 2002; Ting et al., 2003a; Kudryavtseva et al., 2003). The three genes display remarkable amino acid sequence identity with each other, and with *grh*, particularly in the functional DNA-binding and protein dimerization domains (Wilanowski et al., 2002; Ting et al., 2003a). Homologues of this family have also been identified in numerous other species, suggesting conservation of structure and function for over 700 million years (Wilanowski et al., 2002; Ting et al., 2003a; Venkatesan et al., 2003).

The best characterised of the mammalian genes, *Grhl3* plays essential roles in a range of development events. *Grhl3*-null animals exhibit fully penetrant thoraco-lumbo-sacral spina bifida (SB), and co-incident exencephaly in 3% of embryos (Ting et al., 2003b). They also display defective embryonic and adult wound repair, and a failure of skin barrier formation (Ting et al., 2005). This latter role is mediated, in part through the regulation of *transglutaminase 1* (*Tgase1*), an enzyme involved in cross-linking of the epidermal protein/lipid matrix during formation of the impermeable skin barrier (Ting et al., 2005). The mechanisms through which *Grhl3* acts in neural tube closure and wound repair are unknown, although these events share a requirement for epidermal migration, suggesting a role for *Grhl3* in this process.

Consistent with their highly conserved protein-binding domain, biochemical studies had suggested that hetero- and homodimerisation of the *Grhl* factors would be pivotal for their function (Wilanowski et al., 2002). One factor, the LIM-only protein 4 (LMO4) had previously been identified as a putative GRHL3 partner in a yeast-two hybrid screen (Kudryavtseva et al., 2003), and the two proteins had been

* Corresponding author. Rotary Bone Marrow Research Laboratories, C/o Royal Melbourne Hospital Post Office, Grattan Street, Parkville, VIC, 3050, Australia. Fax: +61 3 93428634.
E-mail address: jane@wehi.edu.au (S.M. Jane).

0012-1606/$ – see front matter © 2008 Elsevier Inc. All rights reserved.
doi:10.1016/j.ydbio.2008.06.026

shown to co-immunoprecipitate. LMO4 is a member of the LIM-only subclass of Lim domain proteins and, like GRHL3, plays a role in neural tube development with *Lmo4*-null mice displaying incompletely penetrant exencephaly (50% of embryos) (Hahm et al., 2004; Lee et al., 2005; Tse et al., 2004). An interaction between *Grhl3* and *Lmo4* in epidermal terminal differentiation has previously been reported, where the abnormalities in epidermal histology in the *Grhl3*-null mice were enhanced in the absence of *Lmo4* (Yu et al., 2006). Here, we examine further the biochemical and functional interactions of *Grhl3* and *Lmo4*, establishing cooperative roles for these factors in recognized *Grhl3* functions, and defining and characterising a new cooperative role in eyelid fusion, another paradigm of epidermal migration.

Materials and methods

Mice

Generation and genotyping of *Grhl3*-null mice (*Grhl3*$^{-/-}$) and *Lmo4*-null mice (*Lmo4*$^{-/-}$) was as previously described (Ting et al., 2003b; Lee et al., 2005). *Grhl3*-null and *Lmo4*-null mice were maintained on a C57 Bl/6 and BALB/c background respectively. *Grhl3* and *Lmo4* heterozygous mice were inter-crossed to produce *Grhl3*/*Lmo4* compound heterozygous mice. These offspring were then inter-crossed to produce compound homozygous mice. Noon of the day on which the vaginal plug was detected was taken as embryonic day 0.5 (E0.5) of development following overnight mating. Mice were housed and bred according to standard conditions with food and water ad libitum and were maintained on a 12 h day/night cycle. All animal experiments were pre-approved by The University of Melbourne Animal Ethics Committee.

Histology and electron microscopy

Hematoxylin and Eosin (H&E) staining for histological analysis was performed according to standard protocols. The heads of mice at E11.5, E13.5, E15.0, E15.5 and E16.5 were fixed in 4% paraformaldehyde (PFA)/PBS (10 mM phosphate-buffered saline) overnight at 4 °C and processed for histological analysis as per standard protocols. Embryos to be examined using scanning electron microscopy were fixed overnight at 4 °C in 4% PFA/2.5% glutaraldehyde in PBS and processed as previously reported (Ting et al., 2005).

In situ hybridisation

Embryos were fixed in 4% PFA in PBS at 4°C overnight, embedded in paraffin and sectioned at 7 μm onto gelatin-coated slides. In situ hybridisation was carried out as previously described (Ting et al. 2003b), using 33P-UTP labelled RNA probes corresponding to the unique region of *Grhl3* (nucleotides 404–889) and the entire cDNA of *Lmo4*.

Isolation of mouse keratinocytes and skin barrier analysis

Mouse dorsal skin, collected from E18.5 embryos, was treated with 2.5 mg/ml Dispase and incubated overnight at 4 °C. The epidermis was separated from the dermis and digested in 0.25% trypsin for 10 min. Primary mouse keratinocytes were cultured as previously described (Hager et al., 2004), in low-calcium DMEM medium containing 10% FCS, 100 μg/ml penicillin/streptomycin, 0.25 μg/ml Fungizone and 50 μg/ml gentamycin on vitrogen–fibronectin-coated culture dishes. Skin barrier analysis was performed as previously described (Hardman et al., 1998).

In vitro scratch assays

To analyse the motility of epithelial cells, wildtype and mutant keratinocytes were grown in 6-well culture dishes. Once confluent, the monolayer was 'wounded' using a disposable pipette tip and observed over 24 h for signs of cell migration. For immunostaining, cells were washed twice with PBS and fixed in 4% PFA in PBS for 10 min at room temperature, rinsed again in PBS and processed. Confluent monolayers were then wounded using a disposable pipet tip. Scratches were photographed using a Nikon inverted microscope with attached camera and T-Max400 film at 0 h and 24 h. For immunostaining, keratinocytes seeded onto chamber slides were washed twice with PBS and fixed in 3.7% formaldehyde solution for 10 min at room temperature. F-actins were visualised using Rhodamine–phalloidin at 1:1000 at 4 °C overnight.

Immunofluorescence of actin cable formation

F-actin staining of whole mount eyelids was carried out using eye samples from embryos fixed in 4% PFA in PBS at 4 °C overnight. The anterior portion of the eye, together with surrounding epidermal tissue and intact eyelids, was dissected from fixed tissue and incubated with Rhodamine–phalloidin at 1:1000 and counter-stained with DAPI (1:1000) to visualise nuclei. Samples were then observed with a fluorescence microscope according to standard protocols.

Western Blot analysis and immunohistochemistry

Mouse embryos at E17.5 were collected for the preparation of epidermal protein lysates to analyses by Western blot. Dorsal skin was

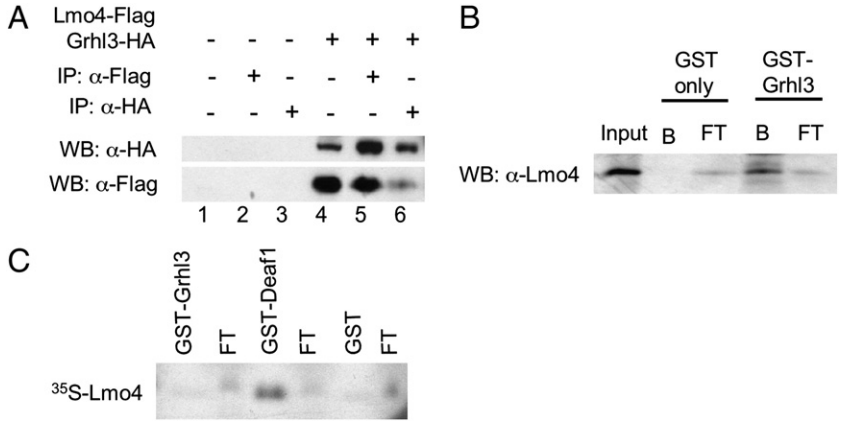

Fig. 1. *Grhl3* and *Lmo4* interact indirectly. (A) Co-immunoprecipitation (IP) analysis of the interaction between GRHL3-HA and LMO4-Flag in 293T cells and immunoblotting (WB) with antibodies against tagged proteins. (B) GST pulldown assay demonstrates that LMO4 derived from cellular extract interacts with GST-GRHL3, but not GST alone B: Glutathione–sepharose beads; FT: Flow through fraction. (C) *In vitro* transcribed/translated ^{35}S-labelled LMO4 interacts with GST-Deaf1, but fails to interact with GST-GRHL3 or GST alone.

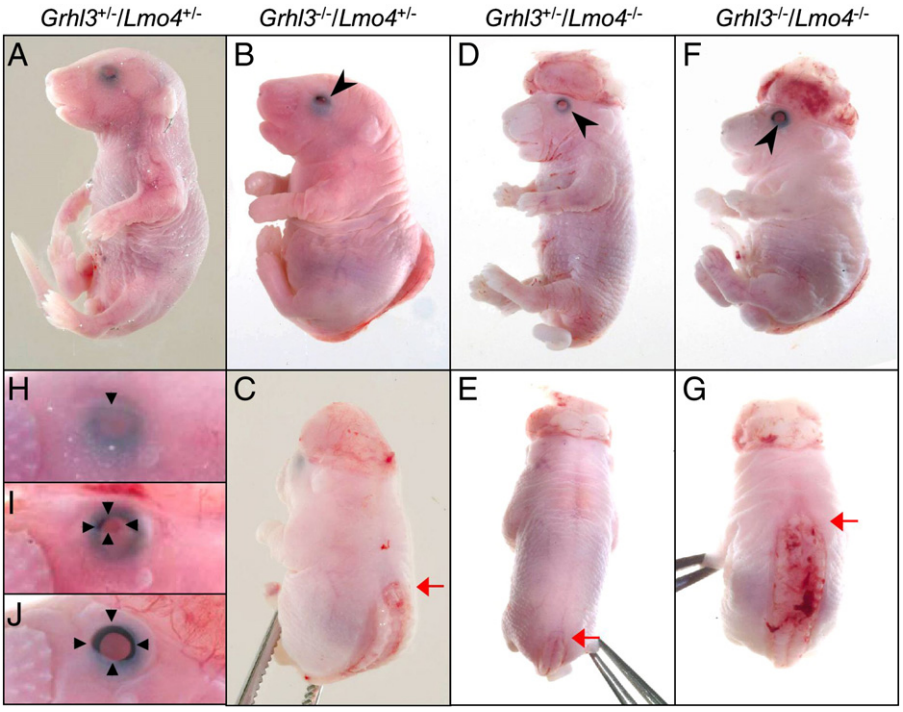

Fig. 2. Phenotypic analysis of *Grhl3/Lmo4* embryos at E18.5. (A, B, D, F) Lateral and (C, E, G) dorsal views of embryos at E18.5 displaying neural tube defects (red arrows) and eyes-open at birth (black arrowheads) in the genotypes indicated. (H–J) Magnified view of eyelids demonstrating varying degrees of closure in: (H) *Grhl3*$^{+/-}$/Lmo4$^{+/-}$; (I) Grhl3$^{+/-}$/Lmo4$^{-/-}$and (J) Grhl3$^{-/-}$/Lmo4$^{-/-}$ E18.5 embryos (black triangles indicate margins of eyelid closure).

removed from these embryos and digested with Dispase to separate the epidermal layer. The epidermis was digested in 0.25% trypsin for 10 min and then lysed in RIPA buffer containing protease inhibitors at 4 °C overnight. Insoluble material was removed by centrifugation. Twenty micrograms of epidermal protein per lane was run on denaturing 10% SDS-PAGE gels and subsequently transferred to PVDF membrane. For blocking and antibody dilution, 5% milk powder (Diploma) in PBS was used. For immunohistochemistry, embryos at time points of interest were collected and fixed in 4% PFA overnight, embedded in paraffin and sectioned at 8 μm onto Superfrost-Plus Slides and processed as per standard protocols using DAB staining. Antibodies used for immunoblotting and immunohistochemistry included Lmo4; c-Jun, p-c-Jun, p-JNK, p38, p-p38, p-ERK (Santa Cruz Biotechnology); p-c-Raf, ERK, MEK1/2, and phospho-MEK1/2 (Cell Signalling). Secondary antibodies included donkey anti-rabbit IgG, donkey anti-goat HRP and sheep anti-mouse IgG conjugated to horseradish peroxidase (HRP) (Amersham Biosciences). For detection of antibodies, the ECL Western Blotting Detection kit (Amersham Biosciences) was used with Amersham Hyperfilm™ ECL. To detect multiple proteins, membrane were treated in stripping buffer (100 mM β-mercaptoethanol, 2% SDS and 62.5 mM Tris, pH 6.8) and reprobed.

Results

GRHL3 and LMO4 interact indirectly

The LIM-domain of LMO4 is a conserved zinc finger motif that confers specificity through protein–protein interactions with DNA-binding proteins in multi-protein complexes (Bach, 2000). To further characterise the biochemical interaction between GRHL3 and LMO4, we initially confirmed that the two proteins could interact in a cellular milieu using co-immunoprecipitation studies. Expression vectors containing hemagglutinin epitope (HA)-tagged *Grhl3* and FLAG-tagged *Lmo4* were co-transfected into 293T cells, and expression of each protein was confirmed with the relevant antiserum (Fig. 1A, lane 4). No signals were observed from untransfected cells (lanes 1–3). Immunoprecipitates from whole cell lysates were obtained with both FLAG (lane 5) and HA antisera (lane 6), and immunoblotted with antisera to both tags. Robust signals were obtained with anti-HA antisera immunoblotting of the FLAG-immunoprecipitate, and also of the anti-FLAG immunoblotting of the HA-immunoprecipitate confirming an interaction between GRHL3 and LMO4 in a cellular context. We then examined their interaction utilizing glutathione *S*-transferase (GST)-chromatography. A GST–GRHL3 fusion protein was coupled to a glutathione–Sepharose matrix and incubated with whole cell extracts from the T47D breast cancer cell line, which expresses LMO4 at high levels. A GST alone matrix served as the control. Bound proteins were eluted and immunoblotted with anti-LMO4 antiserum. A specific interaction was observed with GRHL3, but not with GST alone (Fig. 1B). To determine whether the two proteins interacted directly, ^{35}S-radiolabelled *in vitro* transcribed/translated LMO4 was mixed with GST–GRHL3, and GST alone. A previously identified direct partner of LMO4, DEAF-1 was included as a positive

Table 1
Phenotypic analysis of the genetic interaction between *Grhl3* and *Lmo4*

Grhl3	Lmo4	% of Total	% NAD	% CT	% SB	% EX	% EOB
−/−[a]				100	100	3	0
	−/−[b]					50	0
+/+	+/+	8.8	100				
+/+	+/−	13.5	100				
+/+	−/−	2.6	42			58	14
+/−	+/+	13.1	100				
+/−	+/−	20.1	100				
+/−	−/−	12.0	30	24	18 (L/LS)	70	54
−/−	+/+	7.3	0	100	100 (TLS)	60	25
−/−	+/−	14.2	0	100	100 (TLS)	67	31
−/−	−/−	8.4	0	100	100 (TLS)	100	100

(NAD: no abnormality detected; CT: curly tail, SB: spina bifida; EX: exencephaly; EOB: eyes-open at birth; S: sacral; LS: lumbo-sacral; TLS: thoraco-lumbo-sacral).
[a] On C57 Bl/6 background.
[b] On BALB/c background.

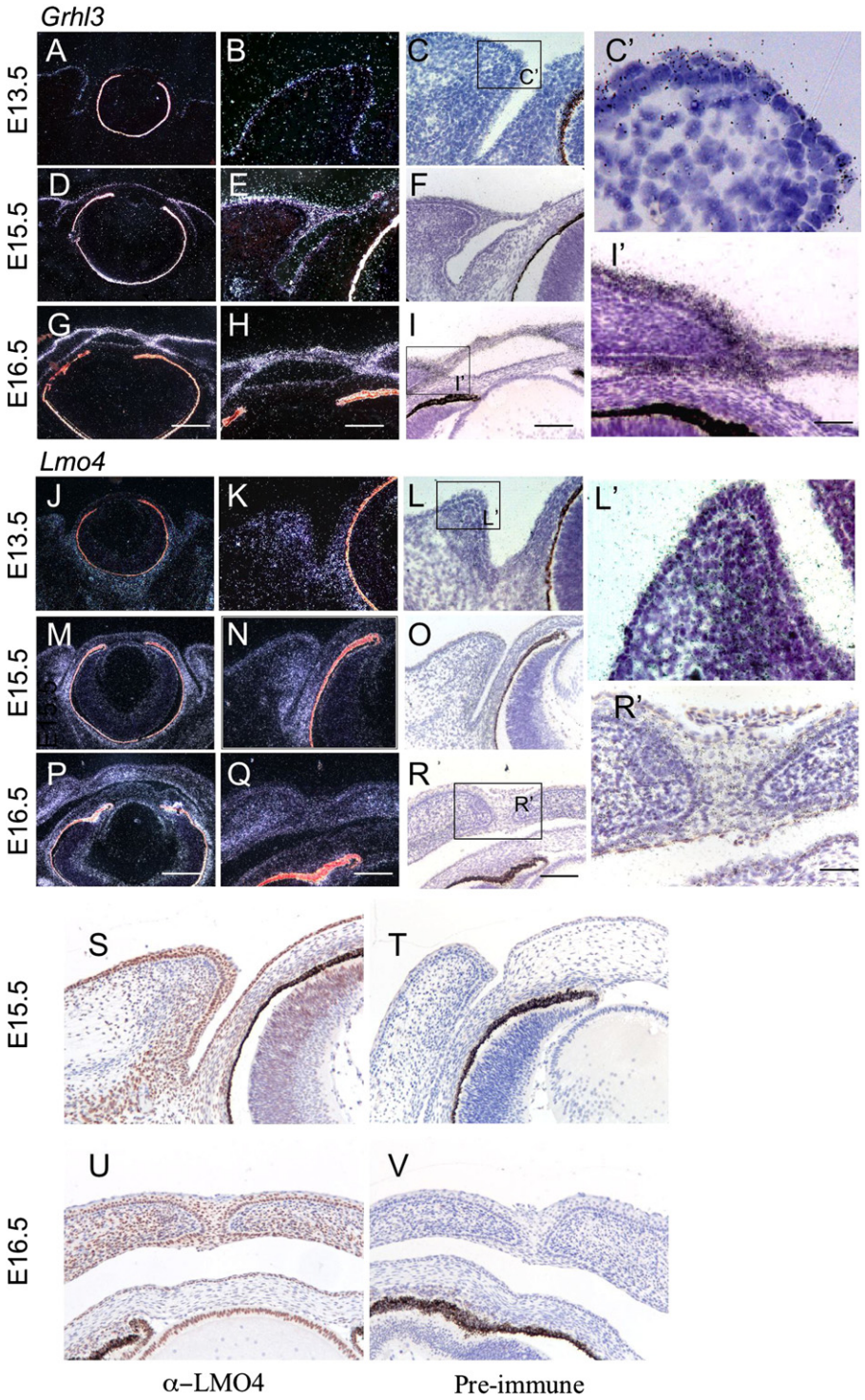

Fig. 3. Expression of *Grhl3* and *Lmo4* during eyelid formation in wildtype mice. In situ hybridisation of the developing eyelid in bright-field (C, F, I, L, O, R) and dark-field (A, B, D, E, G, H, J, K, M, N, P, Q). At E13.5 *Grhl3* is expressed in the ectoderm of the eyelid primordia (A–C). At E15.0 *Grhl3* expression is maintained in the ectoderm and in the leading edge (D–F), where it continues as the opposing sides meet (G–I). At E13.5 *Lmo4* is expressed in the mesoderm immediately surrounding the eye and in the eyelid primordia where it corresponds to a region of dense cell packing (J–L). A similar pattern of *Lmo4* expression is observed at E15.0 (M–O). At E16.5, as the migrating eyelids fuse at the centre of the eye, *Lmo4* is expressed more diffusely in the inner region of the mesoderm and surface ectoderm. (S–V) Immunohistochemistry analysis using an antibody against LMO4 (S, U), and control preimmune sera (T, V) at E15.5 (S, T) and E16.5 (U, V). Scale bars: 20 μm (A, D, G, J, M, P); 4 μm (B, C, E, F, H, I, K, L, N, O, Q, R, S–V); 2 μm (C′, I′. L′, R′).

control (Sugihara et al., 1998). In contrast to our results with whole cell extract, specific retention of LMO4 to the GST–GRHL3 matrix was not observed, although binding of LMO4 to GST-DEAF-1 was demonstrated (Fig. 1C). These findings indicated that GRHL3 and LMO4 do not interact directly, but presumably are components of a multi-protein complex.

Grhl3 and Lmo4 interact genetically in eyelid and neural tube closure

To determine whether the biochemical interaction between GRHL3 and LMO4 had functional consequences during development, we inter-crossed *Grhl3*$^{+/-}$ mice (generated on a C57 Bl/6 background) and *Lmo4*$^{+/-}$ animals (backcrossed onto the BALB/c strain for more

than 10 generations) to generate compound heterozygotes. No developmental abnormalities were observed in either single or compound heterozygous embryos, and all adult animals with these genotypes were healthy and fertile (Fig. 2A and Table 1). *Grhl3*$^{+/-}$/*Lmo4*$^{+/-}$ mice were then inter-crossed and embryos collected at E18.5, as both *Grhl3*$^{-/-}$ and *Lmo4*$^{-/-}$ mice exhibit neural tube defects, and are cannibalised by their mothers at birth. All genotypes were represented in normal Mendelian ratios at E18.5, with the exception of *Grhl3*$^{+/+}$/*Lmo4*$^{-/-}$ (observed: 2.5%; predicted: 6.25%) (Table 1). The phenotypes observed in the *Grhl3*-null and *Lmo4*-null embryos were influenced by the genetic background of the other strain. The incidence of exencephaly increased from 3% in *Grhl3*$^{-/-}$ embryos on the C57 Bl/6 background to 60% on the mixed background, and we observed the emergence of an EOB phenotype (in 25% of *Grhl3*$^{-/-}$/*Lmo4*$^{+/+}$ embryos), that we had never observed in over 1000 *Grhl3*-null embryos generated on the C57 Bl/6 genetic background (Table 1). Similarly, we observed EOB in 14% of the *Lmo4*$^{-/-}$/*Grhl3*$^{+/+}$ embryos on the mixed background that was never observed in more than 500 *Lmo4*-null embryos generated on the BALB/c genetic background. Loss of a single *Lmo4* allele in *Grhl3*-null embryos had a small additional effect on both exencephaly and EOB (Figs. 2B, C and Table 1), whereas loss of a single *Grhl3* allele in *Lmo4*-null embryos led to increased penetrance of the exencephaly (58% to 70%) and EOB phenotypes (14% to 54%), and the emergence of curled tail and SB phenotypes that were never observed in *Lmo4*$^{-/-}$/*Grhl3*$^{+/+}$ or *Lmo4*$^{+/-}$/*Grhl3*$^{+/-}$ embryos (Figs. 2D, E and Table 1). However, only *Grhl3*/*Lmo4* double knockout mice displayed fully penetrant exencephaly, thoraco-lumbo-sacral SB and curled tail, and EOB (Fig. 2F and Table 1). These findings were similar to those previously reported (Yu et al., 2006). In addition to the differences in penetrance, the degree to which the eyelids closed was variable between the various mutant lines. In compound heterozygous mice, the eyelids were consistently closed and fused at the midline at E18.5 (Fig. 2H). In *Grhl3*$^{-/-}$/*Lmo4*$^{+/-}$or *Grhl3*$^{+/-}$/*Lmo4*$^{-/-}$mice, eyelids closure occurred to varying degrees, with some mice having closed eyelids while others displayed eyelids (one or both) that remained slightly open at E18.5 (Fig. 2I). In contrast, all *Grhl3*/*Lmo4* double null mice displayed a complete EOB phenotype in both eyes (Fig. 2J).

Grhl3 and Lmo4 expression during eyelid development

Although the expression patterns of *Grhl3* and *Lmo4* in most embryonic tissues have been documented, specific data in the context of eyelid development was not available. We therefore examined *Grhl3* and *Lmo4* expression during mouse eyelid formation using probes specific for each factor (Fig. 3). At E13.5, *Grhl3* expression was detected in the surface ectoderm of the developing eyelid roots (Figs. 3A–C, C′), and persisted at this location as the eyelids migrated across the corneal surface of the eye, particularly in the leading edge cells (Figs. 3D–F). In E16.5 embryos, *Grhl3* expression was maintained in the ectodermal surface of each eyelid, at both the outer and inner surfaces (Figs. 3G–I, I′), and this persisted at later stages (Supplementary Fig. 1). *Lmo4* expression at E13.5 was detected in a discrete zone around the eye, which included the mesenchyme of the protruding eyelid folds, and a small margin around the sides and back of the eye (Figs. 3J–L, L′). This expression pattern correlates to a region of dense cell packing (Figs. 3L, L′). At E15.5, expression of *Lmo4* was found in the mesenchymal zone of the developing eyelids, as well as the surface ectoderm of the migrating eyelid root where it overlaps with *Grhl3* (Figs. 3M–O). At E16.5, expression was observed in the ectoderm immediately at the point of fusion of the two eyelids at the centre of the eye (Figs. 3P–R, R′). After fusion was completed, *Lmo4* expression in this region was significantly reduced (Supplementary Fig. 1).

We also examined expression of the LMO4 protein during eyelid closure using immunohistochemistry (Figs. 3S–V). At E15.5, robust staining was observed in the ectoderm and underlying mesenchyme, and at E16.5 expression was detected at the point of fusion and elsewhere. We were unable to perform analogous experiments for GRHL3, as our five GRHL3-specific antibodies (3 polyclonal and 2 monoclonal), and several commercial GRHL3 antibodies, did not detect the endogenous protein using immunohistochemistry or immunofluorescence.

Grhl3/Lmo4-null mice exhibit failed eyelid epithelial migration

To further characterise the defects in eyelid fusion in the *Grhl3*$^{-/-}$/*Lmo4*$^{-/-}$ mice, we examined the process morphologically at sequential

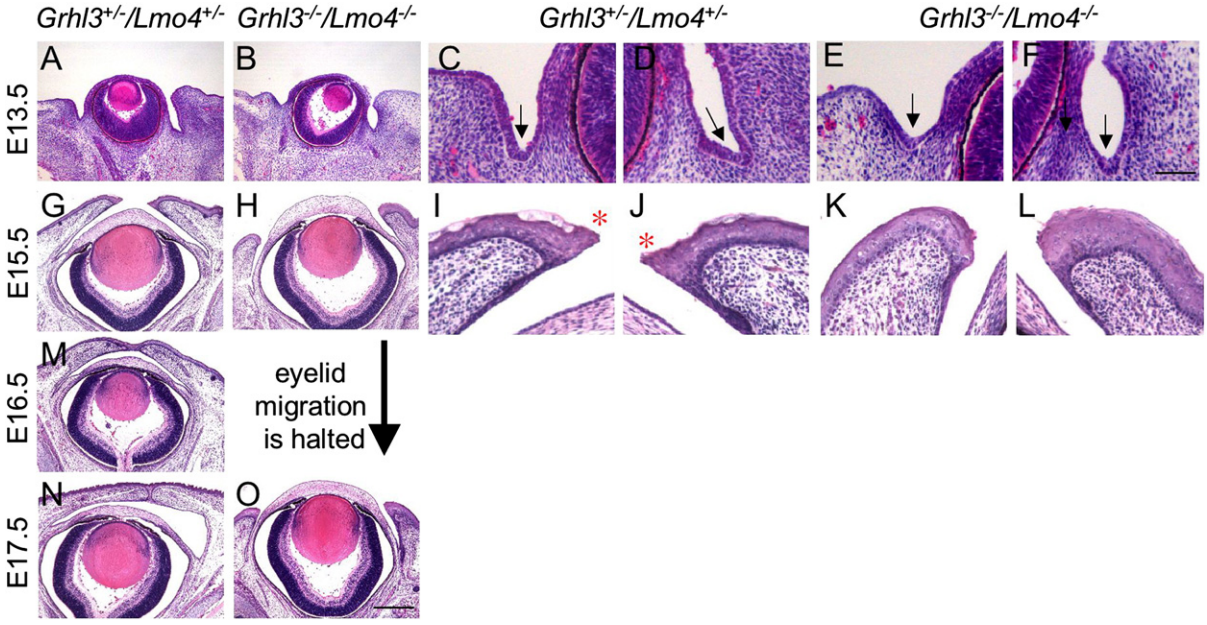

Fig. 4. Eyelid defects in *Grhl3*$^{-/-}$/*Lmo4*$^{-/-}$mice. (A–O) H&E staining of the coronal eye sections from *Grhl3*$^{+/-}$/*Lmo4*$^{+/-}$ (A, C, D, I, J) and *Grhl3*$^{-/-}$/*Lmo4*$^{-/-}$ (B, E, F, K, L, O) embryos. The upper and lower eyelids are at the left and right respectively. Eyelids at E13.5 (A–F), E15.5 (G–L), E16.5 (M) and E17.5 (N, O). (C–F) The arrows indicate the developing eyelid grooves. (I–L) The leading edge beginning to extend across the eye can be seen in *Grhl3*$^{+/-}$/*Lmo4*$^{+/-}$ (*) but not *Grhl3*$^{-/-}$/*Lmo4*$^{-/-}$eyelids. Scale bars: 20 μm (A, B, G, H, M, N, O); 6 μm (C–F; I–L).

developmental time points in control (*Grhl3*$^{+/-}$/*Lmo4*$^{+/-}$) and mutant embryos. Eyelid formation during mouse embryogenesis initiates at E11.5, when the ectodermal grooves form on either side of the eye. At E13.5 mesenchymal protrusions begin to form the new eyelid roots that extend towards the centre of the eye. Between E14.5–E.16.5, a ridge of epithelial cells begins to form at the apex of the nascent upper and lower eyelids, and subsequently extends across the surface of the eye, while the mesenchymal root tracks behind. Fusion only occurs between the epithelium of the upper and lower eyelid, while the mesenchymal tissue remains separate in preparation for re-opening of the eyelids approximately two weeks after birth (Findlater et al., 1993). In control embryos, groove formation and the appearance of mesenchymal protrusions (Figs. 4A, C, D), epithelial migration (Figs. 4G, I, J), and fusion (Figs. 4M, N) proceeded normally. Ectodermal groove formation, and the appearance of mesenchymal protrusions also occurred normally in the *Grhl3*$^{-/-}$*Lmo4*$^{-/-}$ embryos (Figs. 4B, E, F). In contrast, epithelial migration, and consequently eyelid fusion were never observed in the mutants (Figs. 4H, K, L). The timing and site of the failure of eyelid development in the mutants, coincides with the timing and site of *Grhl3* and *Lmo4* co-expression in the wildtype embryos, suggesting that loss of both factors is a critical feature of the EOB phenotype. This is supported by the lack of this phenotype in the

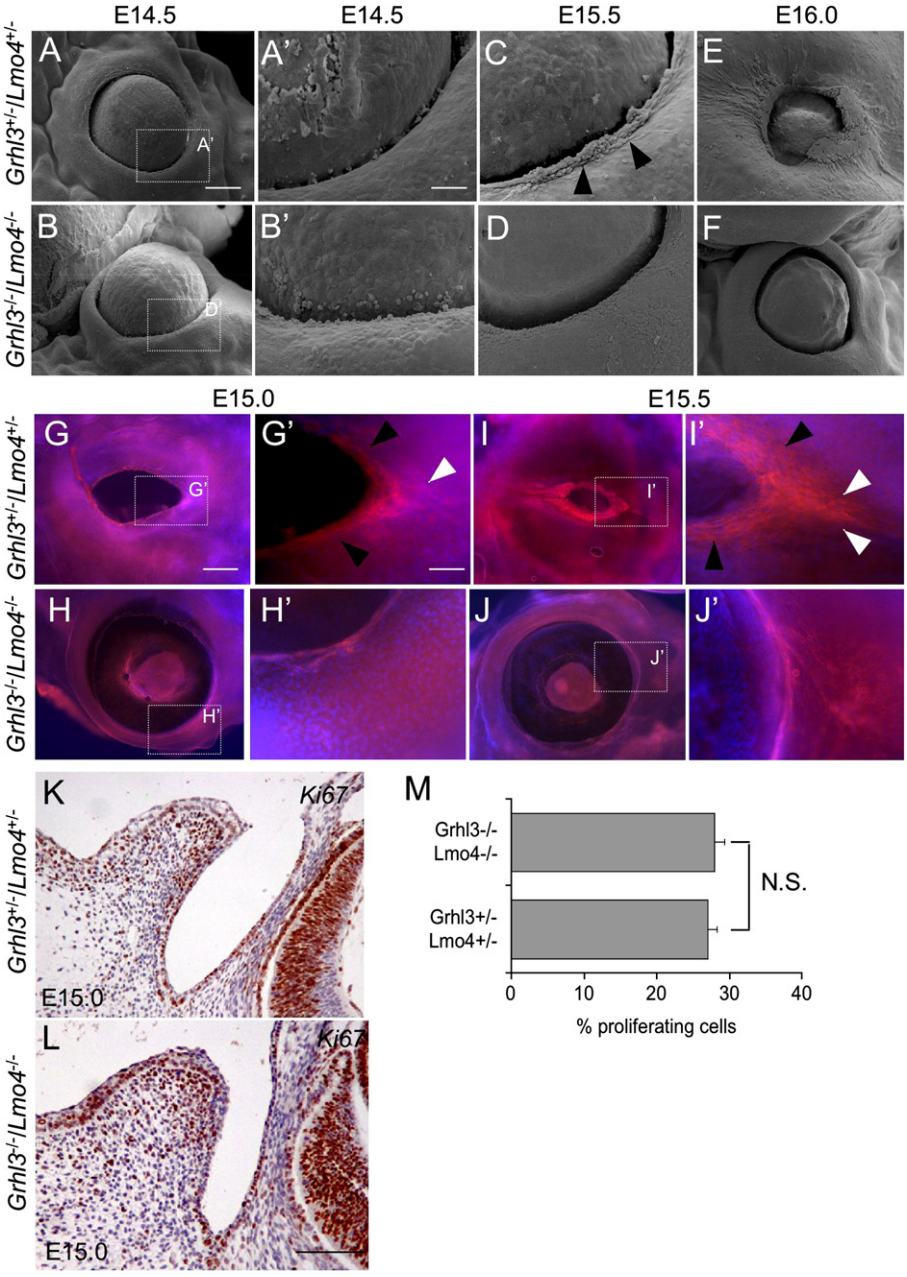

Fig. 5. Leading edge formation and F-actin polymerisation is impaired in eyelid development of *Grhl3/Lmo4* null mice. (A–F) Scanning electron micrographs (SEM) of developing eyelids of *Grhl3*$^{+/-}$/*Lmo4*$^{+/-}$ (A, C, E) and *Grhl3*$^{-/-}$/*Lmo4*$^{-/-}$ embryos (B, D, F). At E14.5 (A, B) no difference is apparent, but at E15.5 (C, D) clumps of peridermal cells are clearly present at the eyelid margin (black arrowheads) of *Grhl3*$^{+/-}$/*Lmo4*$^{+/-}$ (C) but are absent in the *Grhl3*$^{-/-}$/*Lmo4*$^{-/-}$ eyelid (D). Continuous streaming of epithelial cells towards the eyelid margins continues at E16.0 in *Grhl3*$^{+/-}$/*Lmo4*$^{+/-}$ embryos (E) but no further epithelial migration is apparent in *Grhl3*$^{-/-}$/*Lmo4*$^{-/-}$ embryos (F). (G–J) Whole-mount staining of *Grhl3*$^{+/-}$/*Lmo4*$^{+/-}$ (G, I) and *Grhl3*$^{-/-}$/*Lmo4*$^{-/-}$ (H, J) at E15.0 (G, H) and E15.5 (I, J) was carried out using rhodamine–phalloidin and DAPI to visualise F-actin and DNA, respectively. Higher magnification views of boxed areas in G–J are shown in panels G′–J′ respectively. Actin fiber formation (black arrowheads) and radial F-actin cable (white arrowheads) are most prominent in *Grhl3*$^{+/-}$/*Lmo4*$^{+/-}$ eyelids. (K–M) Cellular proliferation is unaffected in *Grhl3/Lmo4* null eyelids. Ki67 staining of *Grhl3*$^{+/-}$/*Lmo4*$^{+/-}$ (K) and *Grhl3*$^{-/-}$/*Lmo4*$^{-/-}$ (L) eyelids at E15.0 show no significant difference in the number of proliferative cells (M). Scale bars: 200 μm (A, B, E–J); 65 μm (A', B', C, D, G'–J'); 4 μm (K, L). N.S. is not significant.

individual mutant lines. These findings also suggest that although *Grhl3* and *Lmo4* may not be required for the initiation of eyelid formation, these genes play important development roles in the process of eyelid closure.

Leading edge extension and actin polymerisation during eyelid closure requires Grhl3 and Lmo4

As the defect in eyelid closure in the mutant mice appeared to predominantly center on failed migration of the leading edge surface ectodermal cells, we employed scanning electron microscopy (SEM) to examine this in more detail (Fig. 5). Consistent with our morphological data, the appearance of the developing eyelids at E14.5 in *Grhl3*$^{+/-}$/*Lmo4*$^{+/-}$ (Figs. 5A, A′) and *Grhl3*$^{-/-}$/*Lmo4*$^{-/-}$ embryos (Figs. 5B, B′) was identical. At E15.5 differences between the control and mutant embryos were emerging, with clusters of epidermal cells appearing at the margins of the eyelid root in the *Grhl3*$^{+/-}$/*Lmo4*$^{+/-}$ mice (Fig. 5C) that were not observed in the *Grhl3/Lmo4* double null mice (Fig. 5D). Twelve hours later, these cells had migrated further towards the center of the eye in the controls (Fig. 5E), but were yet to appear in the *Grhl3*$^{-/-}$/*Lmo4*$^{-/-}$ embryos (Fig. 5F). These results support the hypothesis that the EOB phenotype relates specifically to failed epidermal migration in the mutant mice.

A hallmark of eyelid closure is the formation of an actin cable at the leading edge of epidermal migration, coupled with actin polymerisation and stress fiber formation more laterally (Zhang et al., 2003; Xia and Karin, 2004). Using whole-mount rhodamine–phalloidin staining as a marker of actin polymerisation, we examined actin cable formation in the control and mutant embryos. At E15.0, differences between the *Grhl3*$^{+/-}$/*Lmo4*$^{+/-}$ and the *Grhl3*$^{-/-}$/*Lmo4*$^{-/-}$ embryos were already apparent, with eyelid progression and F-actin polymerisation in the leading edge significantly advanced in the *Grhl3*$^{+/-}$/*Lmo4*$^{+/-}$ eyelids (Figs. 5G, G′) compared to the mutants (Figs. 5H, H′). This difference was even more evident at E15.5, with continued eyelid closure and progressive actin cable formation at the leading and radial margins in *Grhl3*$^{+/-}$/*Lmo4*$^{+/-}$ eyelids (Figs. 5I, I′) in stark contrast to the weak phalloidin staining observed in *Grhl3*$^{-/-}$/*Lmo4*$^{-/-}$ eyelids (Figs. 5J, J′). These data indicate a role for *Grhl3* and *Lmo4* in the regulation of F-actin cable formation at the leading edge of the eyelid, which appears to be linked to epithelial migration and eyelid closure.

To determine whether a proliferation defect was also contributing to the failed eyelid closure in *Grhl3*$^{-/-}$/*Lmo4*$^{-/-}$ embryos, we examined the number of proliferating cells in eyelids of control and mutant embryos at E15.5. Ki67-positive cells (a marker of proliferation) were present in the dermal region of the eyelid root and epithelial cells of the groove region and outer edge (Figs. 5K, L), but there was no significant difference between percentage of Ki67-positive cells in *Grhl3*$^{+/-}$/*Lmo4*$^{+/-}$ and *Grhl3*$^{-/-}$/*Lmo4*$^{-/-}$ eyelids (Fig. 5M). These results indicate that *Grhl3* and *Lmo4* do not impact on cellular proliferation in the context of eyelid formation.

ERK phosphorylation is disrupted in Grhl3$^{-/-}$/*Lmo4*$^{-/-}$*eyelid epithelia*

Studies of the EOB phenotype in mice have demonstrated that eyelid closure requires several signalling pathways, including those involving TGFβ/activin-MEKK1-JNK/p38 and TGFα/EGFR-ERK (Xia and Kao, 2004). To investigate the molecular mechanisms underlying *Grhl3/Lmo4*-mediated eyelid closure, we examined the expression of members of the two pathways in the leading edge of the eyelid at E15.0 using immunohistochemistry. As shown in Fig. 6, ERK (A, B), p38 (E, F), and c-Jun (I, J) were all detected throughout the epithelium and mesenchyme of both the *Grhl3*$^{+/-}$/*Lmo4*$^{+/-}$ and *Grhl3*$^{-/-}$/*Lmo4*$^{-/-}$ eyelid tips. Similarly, the phosphorylated forms of p38 (p-p38)(G, H), and c-Jun (p-c-Jun)(K, L) were also abundant in both epithelial and mesenchymal cells. In contrast, phosphorylated ERK (p-ERK) was robustly expressed in the epithelial layer of the *Grhl3*$^{+/-}$/*Lmo4*$^{+/-}$ eyelids, but was completely absent in these cells in the *Grhl3*/*Lmo4* double null eyelids (Figs. 6C, D). As MEK1/2 are the only known activators of ERK1/2 (Schaeffer and Weber, 1999; Scholl et al., 2007), we examined whether expression of the phosphorylated forms of these proteins was also altered in the *Grhl3*$^{-/-}$/*Lmo4*$^{-/-}$ eyelids (Figs. 6M, N). (Figs. 6M, N). Surprisingly, we observed no difference in expression levels or protein localisation of p-MEK1/2, suggesting the presence of an alternate *Grhl3/Lmo4*-dependent mechanism of ERK activation.

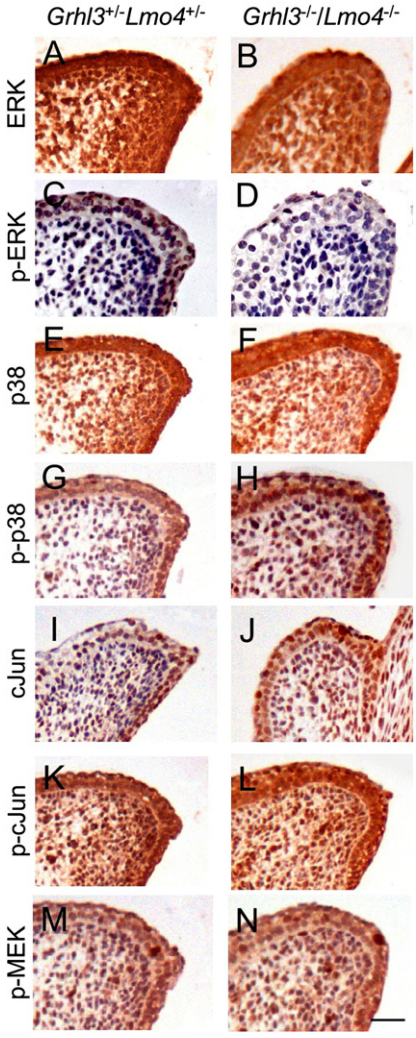

Fig. 6. Activated ERK is reduced at the leading edge of *Grhl3/Lmo4* null eyelids. (A–N) Immunohistochemistry analysis of *Grhl3/Lmo4* double heterozygous and *Grhl3/Lmo4* null eyelids at E15.0 using antibodies against members of the TGFα/EGFR/ERK and TGFβ/activin/JNK pathways, as indicated. Scale bars: 4 μm

Directional motility is disrupted in Grhl3/Lmo4-null keratinocytes

The developmental roles of *Grhl3* and *Lmo4* in neural tube closure and eyelid fusion, two processes involving epidermal migration, suggested that the defects we observed in eyelid may be generalised in all keratinocytes involved in directional migration. To address this, we cultured primary keratinocytes from mutant embryos, and employed an *in vitro* scratch assay to assess the ability of these cells to migrate over a 'wound'. Previous studies had shown that *Grhl3*$^{-/-}$ keratinocytes failed to migrate into the scratched area, whereas *Grhl3*$^{+/-}$ keratinocytes displayed normal movement to 'heal' the 'wounds' within 24 hhours (Ting et al., 2005). We examined whether the loss of one or both alleles of *Lmo4* in keratinocytes heterozygous for the targeted *Grhl3* allele would affect the ability of these cells to migrate. Cultured *Grhl3*$^{+/-}$/*Lmo4*$^{+/-}$ keratinocytes

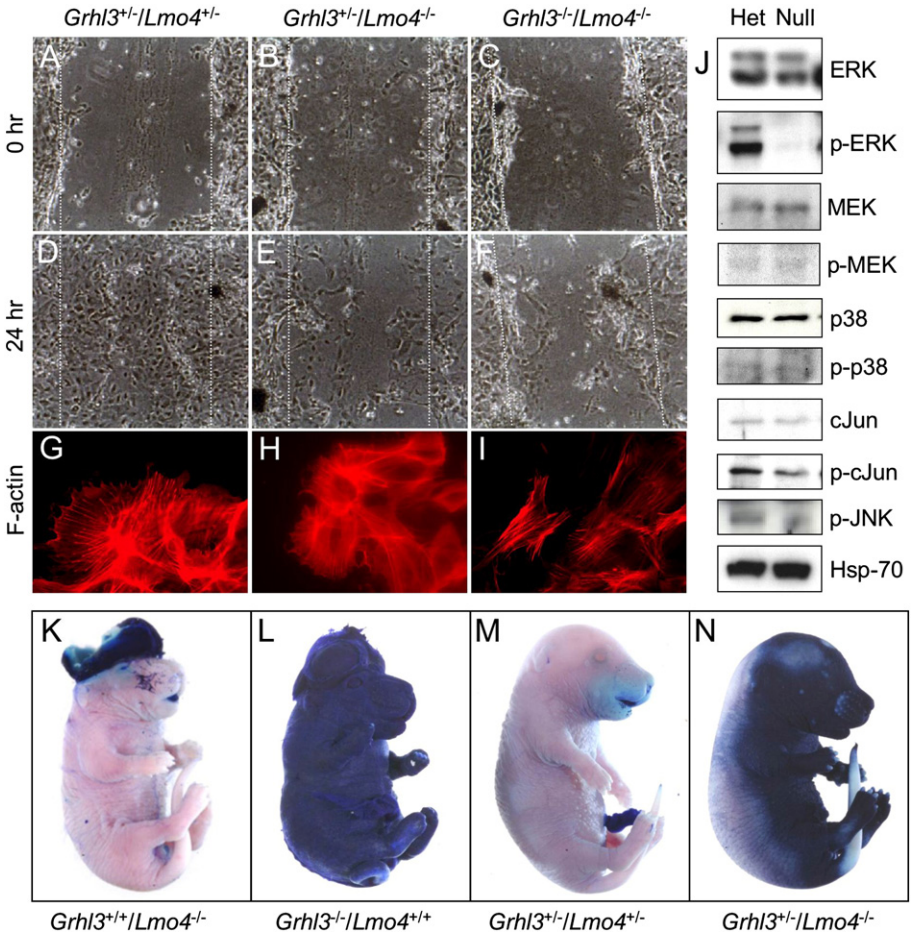

Fig. 7. Migration and actin stress fiber formation are altered in *Grhl3/Lmo4* null keratinocytes. (A–F) *In vitro* wound assays of cultured keratinocytes at 0 h (A–C), and 24 h (D–F) following wounding (dotted line indicates edge of wound). (G–I) Phalloidin-staining of F-actin cable formation in primary keratinocyte cultures. (J, L) Western blot analysis of epidermal protein lysates with antibodies as listed. (K–N) Analysis of barrier formation in embryos of the indicated genotypes at E18.5.

retained the ability to migrate across the introduced 'wound' and completely 'heal' in a 24-hour period (Figs. 7A, D). In contrast, *Grhl3*$^{+/-}$/*Lmo4*$^{-/-}$ keratinocytes were unable to migrate as an epithelial sheet, with many keratinocytes at the front edge losing cellular contact and directed migration (Figs. 7B, E). As expected, this migratory defect was also observed with the *Grhl3*$^{-/-}$/*Lmo4*$^{-/-}$ cells (Figs. 7C, F). Phalloidin-staining of F-actin fibers revealed that *Grhl3*$^{-/-}$/*Lmo4*$^{-/-}$ keratinocytes formed rudimentary stress fibers that showed irregular organization and were not directed towards the gap, as they were in the *Grhl3*$^{+/-}$/*Lmo4*$^{+/-}$ cells (compare Figs. 7I and G). Actin fiber organization in the *Grhl3*$^{+/-}$/*Lmo4*$^{-/-}$ cells was less dramatically affected than the double null cells, but still displayed defects in formation of filopodia and membrane ruffles (Fig. 7H).

In view of these defects in keratinocyte migration, we examined whether the loss of p-ERK expression observed in the leading edge cells in the context of failed eyelid closure in the *Grhl3*$^{-/-}$/*Lmo4*$^{-/-}$ embryos was also evident in the developing epidermis (Fig. 7J). Protein lysates prepared from the dorsal epidermis of E17.5 embryos were analyzed by Western blot, and demonstrated a marked reduction in p-ERK levels, with no change in the levels of the non-phosphorylated form of the protein, or the loading control, Hsp-70. Consistent with our studies in the eyelid, the levels of phosphorylated and non-phosphorylated forms of MEK and p38 were unaltered between the *Grhl3*$^{+/-}$/*Lmo4*$^{+/-}$ and *Grhl3*$^{-/-}$/*Lmo4*$^{-/-}$ epidermis, and the levels of p-c-Jun were marginally decreased in the double null skin. Expression of p-JNK was also unchanged.

To determine whether *Lmo4* and *Grhl3* also functioned co-operatively in the context of barrier formation, embryos harvested at E18.5 (when the barrier is normally fully established) were immersed in toludine blue, and their ability to exclude the dye was assessed. Changes in dye penetration reflect differences in the rates of embryonic acquisition of barrier function (Hardman et al., 1998). As observed previously, embryos lacking *Grhl3* (*Lmo4*$^{+/+}$/*Grhl3*$^{-/-}$) exhibited a profound barrier defect (Ting et al., 2005) (Fig. 7L). In contrast, in embryos lacking *Lmo4* alone (*Lmo4*$^{-/-}$/*Grhl3*$^{+/+}$), the barrier was fully established at E18.5, with only staining of the exposed cerebrum observed (Fig. 7K). *Lmo4*$^{+/-}$/*Grhl3*$^{+/-}$ embryos displayed a slight, but reproducible delay in completion of the barrier, with increased dye penetration in the oro-nasal region, consistent with a functional interaction between the factors in barrier formation (Fig. 7M). This defect was markedly accentuated with loss of the additional *Lmo4* allele, with *Lmo4*$^{-/-}$/*Grhl3*$^{+/-}$ embryos exhibiting a severe barrier defect that was similar to that observed in *Grhl3*-null mice.

Discussion

We report a biochemical and functional interaction between *Grhl3* and *Lmo4* during a range of developmental epidermal morphogenetic events, including neural tube closure and eyelid fusion. Mice deficient for both *Grhl3* and *Lmo4* exhibit fully penetrant exencephaly, thoraco-lumbo-sacral SB, and an EOB phenotype. The two factors also contribute to barrier formation and maintenance, with *Grhl3*$^{+/-}$/*Lmo4*$^{-/-}$ embryos exhibiting marked barrier defects and defective keratinocyte migration. The effects of the GRHL3/LMO4 complex appear to be mediated through the phosphorylated form of ERK1/2, with expression of p-ERK1/2 being lost from both the eyelid epithelium, and the E17.5

epidermis in *Grhl3/Lmo4* mutant mice. As a consequence, actin fiber polymerisation, known to be regulated by ERK signalling, is perturbed, with both diminution and disorganisation of actin bundles in the developing eyelid, and in migrating primary keratinocytes in culture. The failure of eyelid fusion appears to result from defects in both actin polymerisation, and migration of the leading edge cells.

Grhl3 is expressed in the epithelial layers of the eyelid epidermis and inner conjunctiva, while *Lmo4* expression is found in the eyelid mesenchyme from the start of eyelid formation in a pattern that is reminiscent of *Fgf10* (Tao et al., 2005). Eyelid formation begins at E11.5 with groove formation and the establishment of the growing root, both of which require epithelial cell proliferation (Li et al., 2003). In contrast, eventual eyelid closure at around E16.5, which is essential to protect the ocular surface and allow normal development after birth (Findlater et al., 1993), requires epithelial cell migration (Li et al., 2003). Initiation of eyelid development in *Grhl3/Lmo4*-null mice was indistinguishable from wildtype mice, with normal groove formation, root growth and proliferation. Later, however, peridermal clump formation at the eyelid margin was impaired and no further extension of the eyelid occurred across the eye. At this stage, the two genes are co-expressed in the normal migrating eyelid epithelium. Previous studies have implicated *Grhl3* in wound healing and demonstrated that *Grhl3*-null keratinocytes are unable to migrate during re-epithelization (Ting et al., 2005). Similarly, ectopic expression of *Lmo4* has been shown to promote epithelial cell motility and migration (Sum et al., 2005). These results, together with the findings of this study, suggest that *Grhl3* and *Lmo4* are not necessary for cell proliferation, but are required for cell migration during eyelid closure, and other epidermal morphogenetic events.

Previous studies have defined a role for the TGFα/EGFR signalling pathway in eyelid fusion. Mice lacking the EGFR gene exhibit EOB with 100% penetrance (Miettinen et al., 1995; Sibilia and Wagner, 1995; Threadgill et al., 1995), and 40% of TGFα-deficient animals have partial opening of one or both eyes at birth (Luetteke et al., 1993). HB-EGF knockout mice are born with closed eyes, but exhibit a delay in eyelid fusion during development (Mine et al., 2005). EGFR signalling proceeds through MEK1 and MEK2, the only known activators of ERK1/2, which in turn induce actin polymerisation and stress fiber formation. In the context of eyelid closure and wound repair, stress fibers form an actin purse-string which facilitates epithelial closure (Mandato and Bement, 2001; Martin, 1997; Redd et al., 2004). Recently, combined MEK1/MEK2 loss in the epidermis during development has been shown to abolish ERK1/2 phosphorylation resulting in an EOB phenotype with variable penetrance in newborn animals (Scholl et al., 2007). Interestingly, these mice die perinatally with a severely compromised epidermal barrier, suggesting that the presence of this phenotype in the $Grhl3^{+/-}/Lmo4^{-/-}$ embryos may be due, in part, to loss of p-ERK expression in the skin. Surprisingly, the loss of p-ERK we observed in the context of *Grhl3/Lmo4* deletion was not accompanied by any change in p-MEK1/2 levels or localisation, suggesting the presence of an alternate mechanism of ERK activation in this setting. We observed no direct transcriptional effect of the GRHL3/LMO4 complex on the ERK genes, as expression levels of the unphosphorylated forms of these proteins were unchanged in the double null epidermis. Failed eyelid closure has also been observed in mice carrying mutations in genes of the TGFβ/activin–JNK–c-Jun pathway. Cross-talk has also been demonstrated between pathways, with c-Jun known to induce EGFR and HB-EGF expression (Li et al., 2003; Zenz et al., 2003). Although we observed a modest reduction in p-c-Jun expression in the $Grhl3^{-/-}/Lmo4^{-/-}$ epidermis, this was not evident in the developing eyelid, and expression of p-JNK was unaffected.

In addition to influencing eyelid fusion, we have demonstrated that *Grhl3* and *Lmo4* play a cooperative role in neural tube closure and epidermal barrier formation. The contribution of each gene to these various developmental processes differs significantly. For example, EOB is not a feature of the *Grhl3*-null or *Lmo4*-null mice, but the phenotype is fully penetrant with loss of both genes. In contrast, spinal neural tube closure is dependent on *Grhl3* expression, and loss of *Lmo4* only affects this process in the context of reduced GRHL3 levels. Even then, SB is confined to the lower lumbo-sacral regions, suggesting that other factors cooperate with *Grhl3* to close the thoraco-lumbar cord. Skin barrier formation is defective in mice lacking *Grhl3* alone, and this is due, in part, to reduced levels of the cross-linking enzyme *Tgase1* (Ting et al., 2005), as well as perturbations in the expression other structural proteins and alterations in the epidermal lipid content (Yu et al., 2006). However, in this study we observed severely compromised barrier function in mice carrying one functional *Grhl3* allele. The loss of barrier in this context may be due to co-operativity between the two factors in the regulation of *Tgase1* and other genes involved in barrier formation.

Although parallels have been drawn between the epidermal migration observed in eyelid fusion and neural tube closure, no link has been established between TGFα/EGFR/ERK signalling and neurulation. As discussed, the decrease in p-ERK expression in the eyelid and epidermis provides mechanistic insights into the EOB, and keratinocyte migration defects observed in the *Grhl3/Lmo4* mutants, but other signalling pathways would need to be invoked to explain the role of the two genes in closure of the neural tube. One candidate would be the planar cell polarity pathway (PCP), as mice carrying defects in the several of the core PCP genes exhibit both EOB and neural tube defects (Curtin et al., 2003; Lu et al., 2004; Montcouquiol et al., 2003). In support of this, *Drosophila grh* mutants exhibit wing and hair defects consistent with defective PCP signalling (Lee and Adler, 2004), and *Grhl3/Lmo4*-null mice resemble PCP mutant strains, displaying a shortened body axis and severe rostral and caudal neural tube defects. It remains to be established whether *Grhl3* and/or *Lmo4* demonstrate genetic interactions with PCP genes in either of these epidermal migratory events.

Acknowledgments

We thank Lan Ta, Erik Dressler and members of the WEHI and BIO21 Animal Services Facilities for assistance with the mouse lines. We also thank Lin-lin Zhao for excellent technical assistance. S.M.J. is a Principal Research Fellow of the Australian National Health and Medical Research Council (NHMRC). S.B.T. was supported by the Cancer Council of Australia. The work was supported by Project Grants from the Australian NHMRC, and a Grant from the March of Dimes Foundation.

Note: After the submission of this manuscript, Yu et al., described a role for *Grhl3* alone in formation of the epidermal leading edge during eyelid closure.

Yu, Z., et al., 2008. Grainyhead-like factor Get1/Grhl3 regulates formation of the epidermal leading edge during eyelid closure. Dev Biol., in press.

Appendix A. Supplementary data

Supplementary data associated with this article can be found, in the online version, at doi:10.1016/j.ydbio.2008.06.026.

References

Attardi, L.D., Von Seggern, D., Tjian, R., 1993. Ectopic expression of wild-type or a dominant-negative mutant of transcription factor NTF-1 disrupts normal *Drosophila* development. Proc Natl Acad Sci USA. 90, 10563–10567.

Bach, I., 2000. The LIM domain: regulation by association. Mech Dev. 91, 5–17.

Bray, S.J., Kafatos, F.C., 1991. Developmental function of Elf-1: an essential transcription factor during embryogenesis in *Drosophila*. Genes Dev. 5, 1672–1683.

Bray, S.J., Burke, B., Brown, N.H., Hirsh, J., 1989. Embryonic expression pattern of a family of *Drosophila* proteins that interact with a central nervous system regulatory element. Genes Dev. 3, 1130–1145.

Curtin, J.A., Quint, E., Tsipouri, V., Arkell, R.M., Cattanach, B., Copp, A.J., Henderson, D.J., Spurr, N., Stanier, P., Fisher, E.M., Nolan, P.M., Steel, K.P., Brown, S.D., Gray, I. C., Murdoch, J.N., 2003. Mutation of Celsr1 disrupts planar polarity of inner ear hair cells and causes severe neural tube defects in the mouse. Curr Biol. 13, 1129–1133.

Findlater, G.S., et al., 1993. Eyelid development, fusion and subsequent reopening in the mouse. J Anat. 183, 121–129.

Hager, B., et al., 2004. Long-term culture of murine epidermal keratinocytes. J Invest Dermatol 123, 403–404.

Hahm, K., et al., 2004. Defective neural tube closure and anteroposterior patterning in mice lacking the LIM protein LMO4 or its interacting partner Deaf-1. Mol Cell Biol. 24, 2074–2082.

Hardman, M.J., Sisi, P., Banbury, D.N., Byrne, C., 1998. Patterned acquisition of skin barrier function during development. Development 125, 1541–1552.

Jacinto, A., Woolner, S., Martin, P., 2002. Dynamic analysis of dorsal closure in *Drosophila*: from genetics to cell biology. Dev. Cell 3, 9–19.

Kudryavtseva, E.I., et al., 2003. Identification and characterization of Grainyhead-like epithelial transactivator (GET-1), a novel mammalian Grainyhead-like factor. Dev Dyn 226, 604–617.

Lee, H., Adler, P.N., 2004. The grainy head transcription factor is essential for the function of the frizzled pathway in the *Drosophila* wing. Mech Dev. 121, 37–49.

Lee, S.K., et al., 2005. The LIM domain-only protein, LMO4 is required for neural tube closure. Mol Cell Neurosci 28, 205–214.

Li, G., Gustafson-Brown, C., Hanks, S.K., Nason, K., Arbeit, J.M., Pogliano, K., Wisdom, R.M., Johnson, R.S., 2003. c-Jun is essential for organization of the epidermal leading edge. Dev Cell 4, 865–877.

Lu, X., Borchers, A.G., Jolicoeur, C., Rayburn, H., Baker, J.C., Tessier-Lavigne, M., 2004. PTK7/CCK-4 is a novel regulator of planar cell polarity in vertebrates. Nature 430, 93–98.

Luetteke, N.C., Qiu, T.H., Peiffer, R.L., Oliver, P., Smithies, O., Lee, D.C., 1993. TGF alpha deficiency results in hair follicle and eye abnormalities in targeted and waved-1 mice. Cell 73, 263–278.

Mace, K.A., Pearson, J.C., McGinnis, W., 2005. A *Drosophila* epidermal wound response pathway that repairs the body integument requires the Grainyhead transcription factor. Science 308, 381–385.

Mandato, C.A., Bement, W.M., 2001. Contraction and polymerization cooperate to assemble and close actomyosin rings around *Xenopus* oocyte wounds. J Cell Biol. 154, 785–797.

Martin, P., 1997. Wound healing — aiming for perfect skin regeneration. Science 276, 75–81.

Miettinen, P.J., Berger, J.E., Meneses, J., Phung, Y., Pedersen, R.A., Werb, Z., Derynck, R., 1995. Epithelial immaturity and multiorgan failure in mice lacking epidermal growth factor receptor. Nature 376, 337–341.

Mine, N., et al., 2005. HB-EGF promotes epithelial cell migration in eyelid development. Development 132, 4317–4326.

Montcouquiol, M., Rachel, R.A., Lanford, P.J., Copeland, N.G., Jenkins, N.A., Kelley, M.W., 2003. Identification of Vangl2 and Scrb1 as planar polarity genes in mammals. Nature 423, 173–177.

Ostrowski, S., Dierick, H.A., Bejsovec, A., 2002. Genetic control of cuticle formation during embryonic development of *Drosophila melanogaster*. Genetics 161, 171–182.

Redd, M.J., Cooper, L., Wood, W., Stramer, B., Martin, P., 2004. Wound healing and inflammation: embryos reveal the way to perfect repair. Philos Trans R Soc Lond B Biol Sci. 359, 777–784.

Schaeffer, H.J., Weber, M.J., 1999. Mitogen-activated protein kinases: specific messages from ubiquitous messengers. Mol Cell Biol. 19, 2435–2444.

Scholl, F.A., Dumesic, P.A., Barragan, D.I., Harada, K., Bissonauth, V., Charron, J., Khavari, P.A., 2007. Mek1/2 MAPK kinases are essential for mammalian development, homeostasis, and Raf-induced hyperplasia. Dev Cell 12, 615–629.

Sibilia, M., Wagner, E.F., 1995. Strain-dependent epithelial defects in mice lacking the EGF receptor. Science 269, 234–238.

Sugihara, T.M., Bach, I., Kioussi, C., Rosenfeld, M.G., Andersen, B., 1998. Mouse deformed epidermal autoregulatory factor 1 recruits a LIM domain factor, LMO-4, and CLIM coregulators. Proc Natl Acad Sci USA. 95, 15418–15423.

Sum, E.Y., et al., 2005. Overexpression of LMO4 induces mammary hyperplasia, promotes cell invasion, and is a predictor of poor outcome in breast cancer. Proc Natl Acad Sci USA. 102, 7659–7664.

Tao, H., et al., 2005. A dual role of FGF10 in proliferation and coordinated migration of epithelial leading edge cells during mouse eyelid development. Development 132, 3217–3230.

Threadgill, D.W., Dlugosz, A.A., Hansen, L.A., Tennenbaum, T., Lichti, U., Yee, D., LaMantia, C., Mourton, T., Herrup, K., Harris, R.C., et al., 1995. Targeted disruption of mouse EGF receptor: effect of genetic background on mutant phenotype. Science 269, 230–234.

Ting, S.B., Wilanowski, T., Cerruti, L., Zhao, L.L., Cunningham, J.M., Jane, S.M., 2003a. The identification and characterization of human Sister-of-Mammalian Grainyhead (SOM) expands the grainyhead-like family of developmental transcription factors. Biochem J. 370, 953–962.

Ting, S.B., et al., 2003b. Inositol- and folate-resistant neural tube defects in mice lacking the epithelial-specific factor Grhl3. Nat Med 9, 1513–1519.

Ting, S.B., Caddy, J., Hislop, N., Wilanowski, T., Auden, A., Zhao, L.L., Ellis, S., Kaur, P., Uchida, Y., Holleran, W.M., Elias, P.M., Cunningham, J.M., Jane, S.M., 2005. A homolog of *Drosophila* grainy head is essential for epidermal integrity in mice. Science 308, 411–413.

Tse, E., et al., 2004. Null mutation of the Lmo4 gene or combined null mutation of the Lmo1.Lmo3 genes cases perinatal lethality, and Lmo4 controls neural tube development in mice. Mol Cell Biol 24, 2063–2073.

Venkatesan, K., McManus, H.R., Mello, C.C., Smith, T.F., Hansen, U., 2003. Functional conservation between members of an ancient duplicated transcription factor family, LSF/Grainyhead. Nucleic Acids Res. 31, 4304–4316.

Wilanowski, T., Tuckfield, A., Cerruti, L., O'Connell, S., Saint, R., Parekh, V., Tao, J., Cunningham, J.M., Jane, S.M., 2002. A highly conserved novel family of mammalian developmental transcription factors related to *Drosophila* grainyhead. Mech Dev. 114, 37–50.

Xia, Y., Kao, W.W., 2004. The signaling pathways in tissue morphogenesis: a lesson from mice with eye-open at birth phenotype. Biochem Pharmacol. 68, 997–1001.

Xia, Y., Karin, M., 2004. The control of cell motility and epithelial morphogenesis by Jun kinases. Trends Cell Biol 14, 94–101.

Yu, Z., Lin, K.K., Bhandari, A., Spencer, J.A., Xu, X., Wang, N., Lu, Z., Gill, G.N., Roop, D.R., Wertz, P., Andersen, B., 2006. The Grainyhead-like epithelial transactivator Get-1/Grhl3 regulates epidermal terminal differentiation and interacts functionally with LMO4. Dev Biol. 299, 122–136.

Zenz, R., Scheuch, H., Martin, P., Frank, C., Eferl, R., Kenner, L., Sibilia, M., Wagner, E.F., 2003. c-Jun regulates eyelid closure and skin tumor development through EGFR signalling. Dev Cell 4, 879–889.

Zhang, L., et al., 2003. A role for MEK kinase 1 in TGF-beta/activin-induced epithelium movement and embryonic eyelid closure. EMBO J. 22, 4443–4454.